Article

Prussian Blue Encapsulated with Brush-like Polyorganosiloxane Nanospheres with Tunable Functionality

Yue Chang, Kaimin Chen *, Ziwei Li, Xueke Zhang, Chenming Xu, Jihu Wang and Shaoguo Wen

College of Chemistry and Chemical Engineering, Shanghai University of Engineering Science, Shanghai 201620, China; changyue0507@163.com (Y.C.); v2904602967@163.com (Z.L.); zxk18790756892@163.com (X.Z.); wuke01052001@163.com (C.X.); wangjihu@163.com (J.W.); sgwen1@sues.edu.cn (S.W.)

* Correspondence: kmchen@sues.edu.cn

Abstract: Faced with higher demands of pigments in various applications, the performance of pigments in a specific system is in urgent need of optimization and improvement. Polyorganosiloxane (POS) stands out among various encapsulating polymeric materials for pigment modification due to its superior thermal stability and alkali resistance. However, the inherent hydrophobicity of POS causes poor stability in aqueous systems, which is usually applied in environmentally friendly applications. Grafting hydrophilic polymer chains on the surface of POS could improve water dispersity. In addition, the encapsulated pigment can also be endowed with various functionalities by selecting or combining grafted polymers. Herein, we reported a strategy to encapsulate Prussian blue (PB27) with POS grafted with poly(acrylic acid) (PAA) or poly(N-(2-hydroxyethyl) acrylamide) (PHEAA) to allow better stability and functionality of the composite pigment particles, denoted as PB27@POS@PAA or PB27@POS@PHEAA, respectively. The effect of the number of monomers and the amount of initiator potassium persulfate (KPS) on the brush thickness of the grafted polymers was studied, along with various performance properties and the functionality of PB27@POS@PAA and PB27@POS@PHEAA. The dispersity, alkali resistance, and high-temperature stability are studied. The brush-like composite pigment performs better after centrifugation (5000 rpm, 30 min) or treatment under 90 °C when the dosage of grafting monomer AA or HEAA reaches 400 wt%. Optimal alkali resistance was obtained for PB27@POS@PAA (AA, 200 wt%) with a particle size variation of only 31 nm after 8 h. Comparably, PB27@POS@PHEAA behaved worse under similar conditions. Moreover, PB27@POS grafted with PAA was responsive to pH and that with PHEAA showed excellent antifouling properties, which could also be replaced by other functional monomers if needed.

Keywords: Prussian blue; polyorganosiloxane; poly(acrylic acid); poly(N-(2-hydroxyethyl) acrylamide)

1. Introduction

Pigments are a necessary part of industry and are commonly utilized in various products such as textiles [1], inks [2], coatings [3], and so on. Compared with dyes, pigments have the advantages of strong coloring power [4], complete color spectrum [5], being insoluble in solvents, e.g., water, etc. However, many pigments have some limitations under certain processing conditions (e.g., heat [6], pH [7], light [8], or the presence of other additives [9]), affecting many of their further applications. A variety of pigment modification methods have been developed and applied [10–13]. Among the various strategies, encapsulating the pigment with organic or inorganic materials is a promising method that can potentially protect it from degradation and improve pigment stability [14–16] due to the small migration of pigments from encapsulating materials [17]. In our previous work, pigment yellow 155 (PY155) was encapsulated with poly(methyl methacrylate-co-butyl

acrylate) to solve the problem of stabilizing pigments in aqueous systems [18]. Zhou et al. encapsulated the phthalocyanine pigments with a copolymer of methyl methacrylate (MMA) and butyl acrylate (BA) by a mini-emulsion polymerization method, making these pigments effectively dispersed in water and have good compatibility with the resin [19]. However, it is not adequate to use common polymers to modify the pigments, especially for pigments with poor stability in conditions like high temperature, extreme pH conditions, etc.

Compared to common polymers, polyorganosiloxane (POS) [20], also known as silicone, has attracted increasing attention all over the world owing to its good heat resistance [21], aging resistance [22], chemical stability [23], biocompatibility [24,25], and other outstanding properties [26]. POS was also employed to modify pigments to enhance its performance at high levels. Existing strategies of taking advantage of POS for modifying pigment mainly focus on simply encapsulating with pure POS [27] or POS-modified polyurethane [28] or acrylic coatings [29] on the pigment surface. However, the hydrophobicity of POS is high [30] and when it is used to encapsulate pigments in aqueous systems, the composite particles tend to aggregate and settle, resulting in poor stability.

An alternative method is to graft polymer brushes on the surface of POS. For one, the grafted polymer chains can prevent the pigment hybrids from agglomerating or precipitation through steric hindrance [31] or electrostatic interaction [32]. In comparison to the extra addition of emulsifiers or dispersants, the chemically bonded structure gives the pigment better stability. For another, there are abundant sources of grafted monomers that can be selected or combined flexibly according to practical applications [33,34], which can endow the encapsulated pigment with multiple functions.

Existing methods of grafting polymer chains on the surface of POS are chiefly based on the reactive groups [35] or the silane coupling agent [36] but these traditional routes to graft polymer chains on the surface of POS generally require labor-consuming procedures and have low universality. Exploring an approach with controllability, strong commonality, simplicity, and convenience is urgent.

Prussian blue (PB27), also known as iron blue, is a generally applied inorganic pigment [37,38]. It is also used in the preparation of absorbents for the removal of toxic inorganic ions, particularly radionuclides, from water [39]. Nevertheless, PB27 is extremely thermolabile [40]. Moreover, it usually fades over time in alkaline environments where it is decomposed and becomes visibly discolored [41]. Although PB27 has been used for more than 300 years, the problem of fading and decomposition remains unresolved, whether at high temperatures or in alkaline conditions, leading to limited applications compared to other blue pigments.

Herein, PB27 is selected as the raw pigment and POS is chosen as the encapsulating material. To further improve the comprehensive properties of POS-modified PB27, a simple and versatile heat-initiated grafting method was proposed to graft the functional polymers on the surface of the POS-modified PB27. Acrylic acid (AA) or methyl N-(2-hydroxyethyl) acrylamide (HEAA) is selected as the functional monomers for grafting (Figure 1) [42]. The composite pigment particles were fully characterized by Fourier infrared spectroscopy (FTIR), thermogravimetric analysis (TGA), and transmission electron microscopy (TEM). Various performance properties were carried out for the functional composite pigment particles. Not only were the comprehensive properties of POS-modified PB27 improved but the functionality brought by PAA or PHEAA brush was also confirmed.
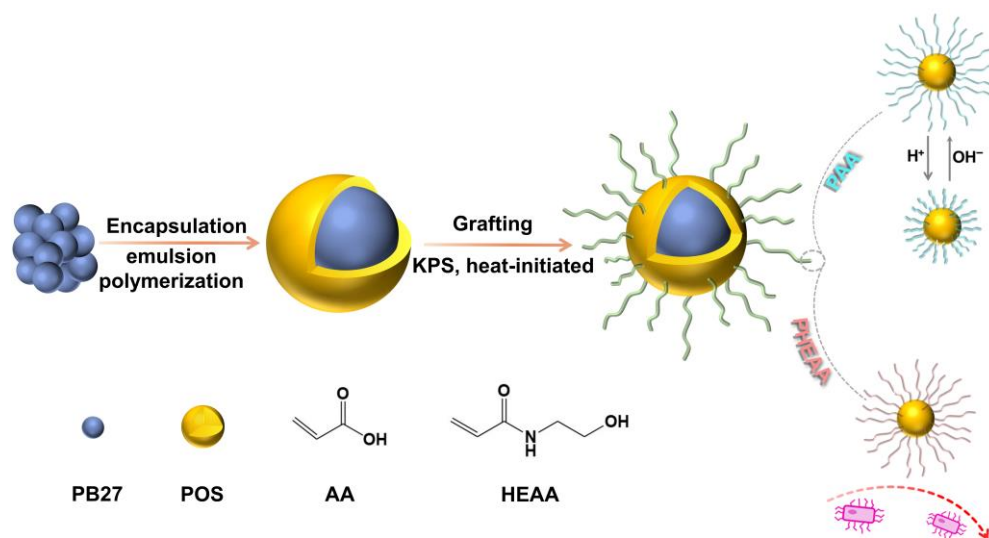
Figure 1. Schematic illustration of the preparation of functional composite pigment particles.

## 2. Materials and Methods

2.1. Materials

Prussian blue (PB27) was supplied by Shanghai Macklin Biochemical Co., Ltd. (Shanghai, China). Methyltrimethoxysilane (MTMS), phenyltrimethoxysilane (PTMS), dimethoxymethylphenylsilane (DMMPS), hexadecane (HD), acrylic acid (AA), and N-(2-hydroxyethyl) acrylamide (HEAA) were bought from Adamas-beta (Shanghai, China). Sodium dodecyl sulfate (SDS) was purchased from Shanghai Titan Technology Co., Ltd. (Shanghai, China). Potassium persulfate (KPS) was provided by Aladdin Industrial Co. (Hangzhou, China). Deionized water was used for all the experiments in this study. AA and HEAA monomers were purified to eliminate the inhibitors and stored in a 4 °C refrigerator before use. All the other chemical reagents used were of analytical grade and utilized without further purification.

2.2. Preparation of PB27@POS

The preparation of PB27@POS particles by encapsulating PB27 with POS is shown in Figure 2 and the formula is shown in Table 1 (Note: the molar ratio of monomers, MTMS, PTMS, and DMMPS, used to synthesize the POS component is 1:1:1). Firstly, the pigment phase, the monomer phase, and the mixture of the two phases were pre-dispersed or preemulsified for 3 min using an ultrasonic processor (Scientz-IID, Ningbo Scientz Biotechnology Co., Ltd., Ningbo, China) at 150 W with 5 s pulse on and 1 s pulse off under ice cooling [18,19]. Next, the mixture phase were transferred into a three-necked flask. Finally, under mechanical stirring of 350 rpm, an HCl solution (1.0 wt%) was added dropwise with a constant pressure funnel at 55 °C and the polymerization was further carried out at 55 °C for another 2 h.

Table 1. The formula for preparing Prussian blue is modified with polyorganosiloxane (PB27@POS).

PB27	SDS	Monomers	HD	HCl (1.0 wt%)	Deionized Water
0.2 g	0.3 g	2.58 g	0.1 g	10.0 g	136.7 g
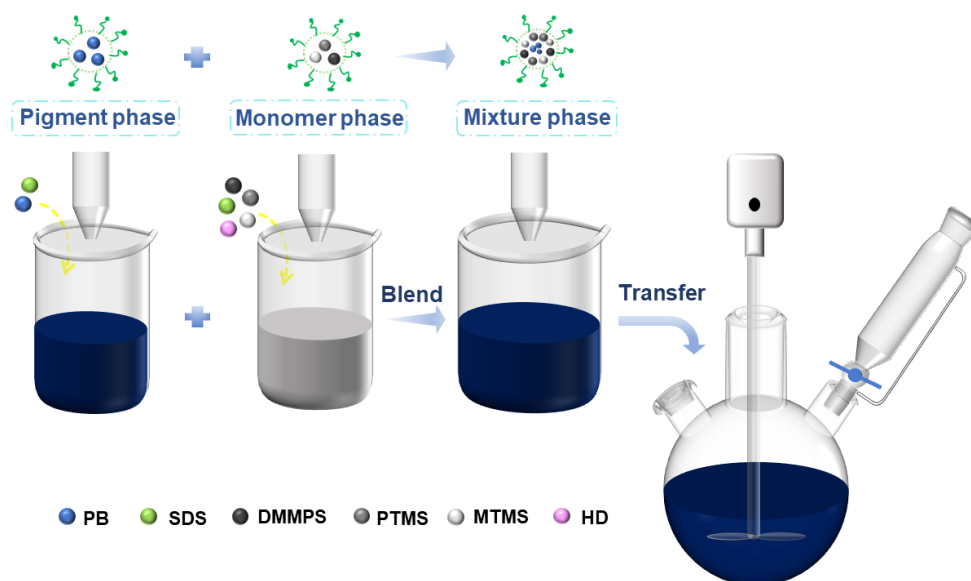
Figure 2. A brief diagram for the synthesis of Prussian blue (PB27) modified with polyorganosiloxane (POS) (PB27@POS).

2.3. Functionality of PB27@POS

Different from our previous work [18,19] using photo-emulsion polymerization, a heat-initiation process was applied in this work. Firstly, KPS and the composite pigment particles of PB27@POS were transferred into a three-necked flask. Next, the functional monomer (AA or HEAA) was added dropwise under nitrogen atmosphere and mechanical stirring (350 rpm) when the oil bath reached 70 °C for 10 min. After the monomer was added completely, the reaction proceeded for another 1.5 h. The formula involved in this process is shown in Table 2. The amount of PB27@POS solution is fixed at 50.0 g with 0.8 g solid in it. The effectiveness of other initiators except KPS is not carried out in this work and needs further investigation.

Table 2. The formula for the polymer grafting on Prussian blue was modified with polyorganosiloxane (PB27@POS).

Number	PB27@POS	KPS	Monomers
1	50.0 g	0.02 g	0.4 g
2	50.0 g	0.02 g	0.8 g
3	50.0 g	0.02 g	1.6 g
4	50.0 g	0.02 g	2.4 g
5	50.0 g	0.02 g	3.2 g
6	50.0 g	0.04 g	1.6 g
7	50.0 g	0.08 g	1.6 g
8	50.0 g	0.10 g	1.6 g

2.4. Characterization

2.4.1. General Characterizations

Fourier Transform–infrared (FTIR) spectra of the composite pigment particles were recorded on a Nicolet iS5 FTIR spectrometer (AVATAR370, PerkinElmer Instruments Co., Ltd., Shelton, CT, USA) over a range of 4000 to 400 cm^{-1}, using the ATR method. Samples were pressed against the diamond crystal for acquirements (32 scans). The morphologies were observed by transmission electron microscopy (TEM, JEOL JEM-2100Plus, JEOL Ltd., Tokyo, Japan) at an operating voltage of 200 kV. The particle size and size distribution (Z-average is for the particle size and the size distribution is calculated from a cumulants

analysis based on G1 correlation function) were measured by dynamic light scattering (DLS) on a Nano-S90 particle sizer (Malvern Instruments Ltd., Worcestershire, UK). TGA was performed by TGA550 (Newcastle, DE, USA). The samples were heated from 30 °C to 800 °C at a heating rate of 10 °C/min under a nitrogen atmosphere.

2.4.2. Performance Characterizations

In terms of thermal stability, the particle sizes and photographs of the samples before and after standing in a 90 °C oven for 1 week were tracked and compared. Moreover, the thermogravimetric analysis (TGA) was also applied to further investigate the thermal properties. For mechanical stability, the photographs and the particle size variation in the samples before and after centrifugation for 30 min at 5000 rpm were compared. As to the alkali resistance, the sample solution (5 mL, 0.02 mg/mL) was mixed fully with 1.0 mL NaOH solution (0.25 M) and left to stand at room temperature. The optical photos and DLS results recorded at regular intervals were applied to analyze the alkali resistance of the composite pigment particles.

2.4.3. Functionality Characterizations

The pH response was carried out by monitoring the size change in PB27@POS@PAA under different pH by a pH meter (Shanghai Leici Instrument Factory, Shanghai, China) and DLS. HCl solution (0.1 M) and NaOH solution (0.1 M) were applied to adjust the pH of PB27@POS@PAA (0.02 mg/mL) dispersed in a phosphate buffer (PB, 1 mM). The pH was continuously tuned from alkaline to acid.

The antifouling property of PB27@POS@PHEAA with different brush thicknesses was studied by the interaction between bovine serum albumin protein (BSA, pI 4.9) and PB27@POS@PHEAA. Both turbidimeter (Shanghai Leici Instrument Factory) and DLS were applied. BSA solution (0.02 mg/mL) was mixed with PB27@POS@PHEAA solution (0.04 mg/mL) and deionized water was added to a beaker. The ionic concentration in this mixture was set as 10 mM. NaOH solution (0.1 M) and HCl solution (0.1 M) were used to adjust the pH value of the commixture from 10 to 3. The turbidity of the mixture at pH 10 was taken as the control.

3. Results and Discussion

3.1. Characterization of the Composite Pigment Particles

The chemical compositions and morphologies of PB27, PB27@POS, PB27@POS@PAA, and PB27@POS@PHEAA were studied by FT-IR and TEM, respectively. As shown in Figure 3, the FT-IR spectrum of PB27 exhibited its characteristic band of -CN around 2030 to 2100 cm^{-1}. The FTIR spectrum of PB27@POS showed the presence of a characteristic band of Si-C at 1258 cm^{-1}, a wide characteristic band of Si-O-Si in the range of 1007 cm^{-1} to 1100 cm^{-1}, and the characteristic bands of C-H at 3050 cm^{-1} and 3070 cm^{-1}. The intensity of the PB27@POS weakened at 2030–2100 cm^{-1} brought by PB27, indicating that POS encapsulated PB27 successfully. In contrast with that of PB27@POS, a new characteristic band located at 1716 cm^{-1} in the spectrum of PB27@POS@PAA was found, which was attributed to the stretching vibration of the C=O present in the carboxyl group of PAA. Furthermore, compared with the spectrum of PB27@POS, characteristic bands of PB27@POS@PHEAA appeared at 1562 cm^{-1}, ascribed to the stretching vibration of C=O, and characteristic bands appeared at 1555 cm^{-1} and 3274 cm^{-1}, ascribed to the bending vibration of N–H belonging to amide groups, which indicated the existence of PHEAA.
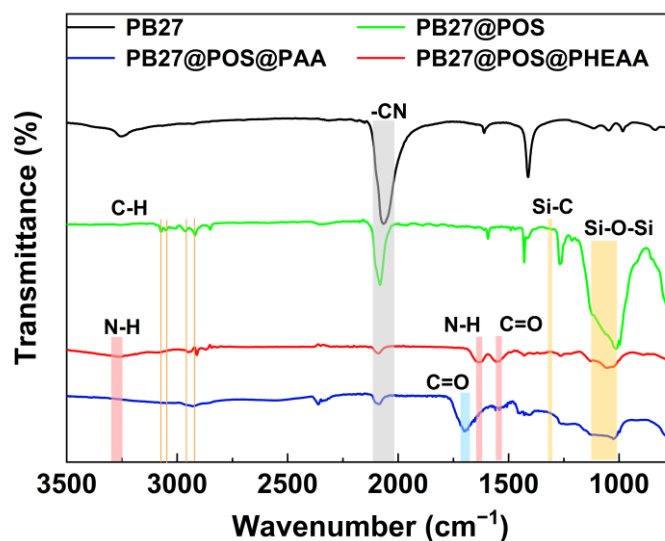
Figure 3. The FT-IR spectra of Prussian blue (PB27); PB27 modified with polyorganosiloxane (POS) (PB27@POS) and grafted with poly(acrylic acid) (PAA) (PB27@POS@PAA) or poly(N-(2-hydroxy-ethyl) acrylamide) (PHEAA) (PB27@POS@PHEAA).

Figure 4a shows the morphology of PB27, which is nearly spherical. The TEM image in Figure 4b demonstrates the morphology of PB27@POS, a core-shell structure could be observed, demonstrating that the PB27 was encapsulated by POS successfully. Figure 4c,d exhibits a more regular spherical shape and an evident core-shell structure for PB27@POS@PAA and PB27@POS@PHEAA, respectively. The DLS results also showed that the particle size was increased by 100 nm after PAA or PHEAA was grafted. The particle size variation further confirms the successful grafting of PAA or PHEAA onto the surface of PB27@POS.
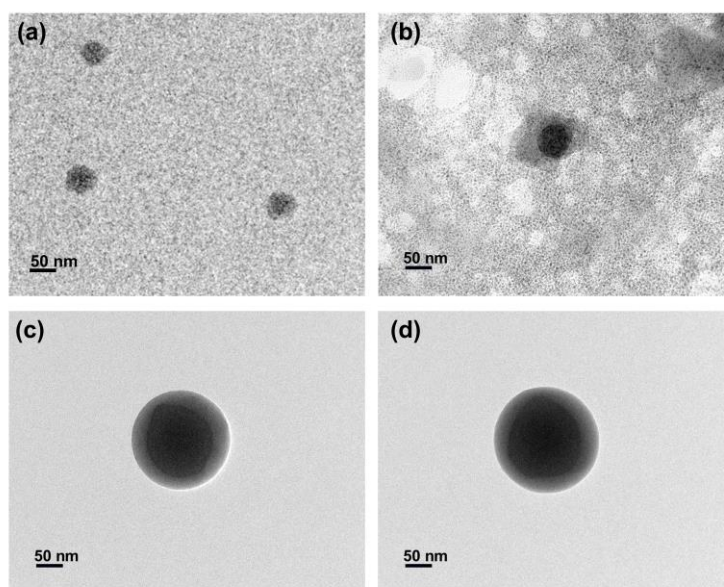
Figure 4. TEM images of (**a**) Prussian blue (PB27), (**b**) PB27 modified with polyorganosiloxane (POS) (PB27@POS), and grafted with (**c**) poly(acrylic acid) (PAA) (PB27@POS@PAA) or (**d**) poly(N-(2-hydroxyethyl) acrylamide) (PHEAA) (PB27@POS@PHEAA).

3.2. The Effect of Monomer Dosage

The influence of the dosage of AA or HEAA on the brush thickness of the composite pigment particles was first studied. As shown in Figure 5, the particle size of PB27@POS@PAA gradually increased from 170 nm to 686 nm and that of PB27@POS@PHEAA gradually rose from 170 nm to 415 nm. The larger the monomer dosage, the bigger the functional composite pigment particles. In addition, not only the particle size of the functional composite pigment particles increased gradually with the increase in monomer dosage but the particle size distribution also widened. Especially when the monomer dosage exceeded 300 wt%, the PDI even was over 0.4 for PB27@POS@PAA, which may be due to possible coupling termination between propagating chains on neighboring nanoparticles.
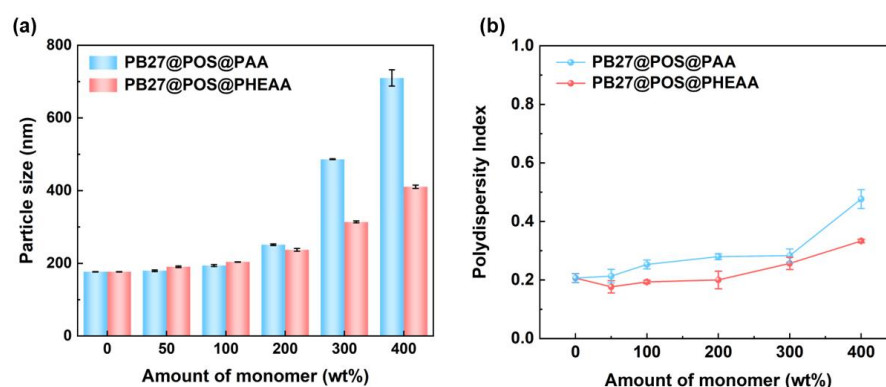
Figure 5. (**a**) Particle size and (**b**) size distribution of the functional composite pigment particles with different monomer dosages.

3.3. The Effect of KPS Dosage

In this work, KPS was the selected initiator and the effect of KPS dosage on the brush thickness of the grafted polymers was investigated. As shown in Figure 6, with the increase in KPS, the particle size of the functional composite pigment particles tended to first increase and then decrease. When the dosage of KPS was 5.0 wt%, the particle size of PB27@POS@PAA and PB27@POS@PHEAA both reached the maximum values. When the amount of KPS was small, the number of free radicals triggered by KPS was consumed by some contaminants or impurities, which affected the effective grafting, leading to the small size of the functional composite pigment particles. With the increase in the amount of KPS, more active sites were formed to be grafted with polymer chains, so the size of the functional composite pigment particles rose. However, as the amount of KPS continued to increase, there were plenty of free radicals in the reaction system, which enhanced the chain termination resulting in a decrease in the particle size. Similarly, the size distribution of PB27@POS@PAA and PB27@POS@PHEAA also tended to first increase and then decrease.
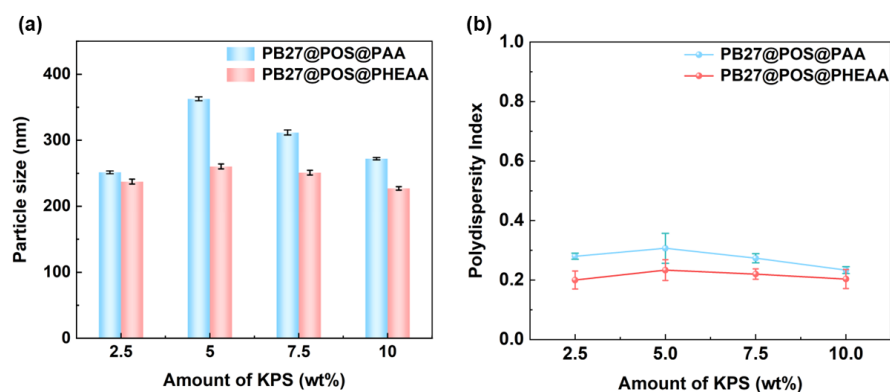
Figure 6. (**a**) Particle size and (**b**) size distribution of the functional composite pigment particles with different potassium persulfate (KPS) dosages.

3.4. Performance Characterizations

3.4.1. Thermostability

The thermostability of PB27 is very important. We not only tracked and compared the particle size of PB27@POS@PAA and PB27@POS@PHEAA with different brush thicknesses but also studied its thermal properties before and after modification by TGA. As shown in Figure 7, when the samples were left to stand at 18 °C for a week, the particle size of all functional composite pigment particles did not change significantly. As for samples left to stand at 90 °C for a week, the particle size of PB27@POS@PAA-50 decreased (notably, the PB27@POS grafted with 50 wt% AA is expressed as PB27@POS@PAA-50, the same below), which was consistent with the settlement of the sample. The particle size of others all increased obviously at 90 °C. In addition, there was no apparent settlement for PB27@POS@PHEAA-50 standing at 90 °C and its particle size rose rather than decreased. It is probably attributed to the thicker polymer brushes than that of PB27@POS@PAA-50. The optical photos for the above stability study were shown in the supporting information (Figure S1).
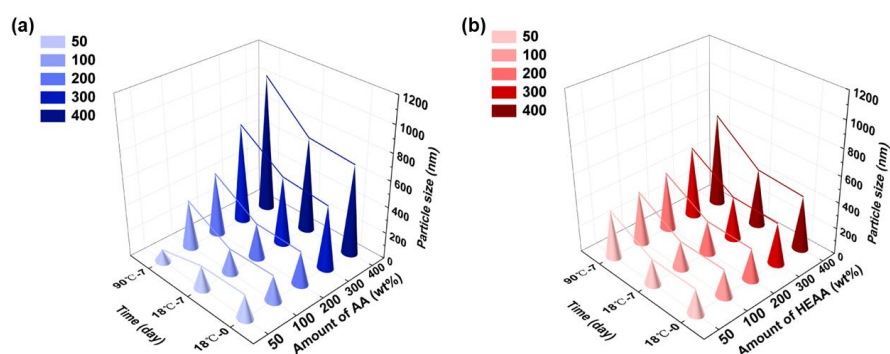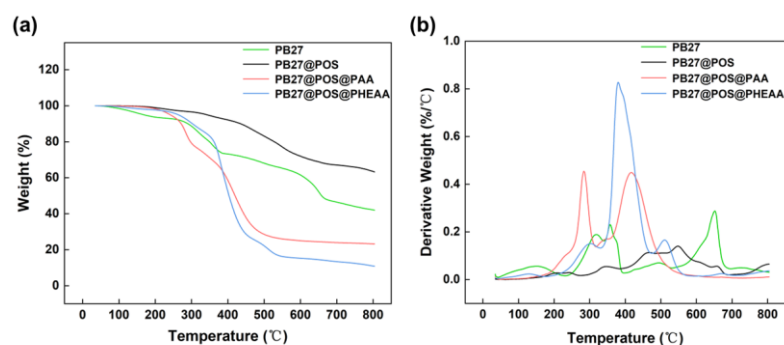

Figure 7. The size variation in Prussian blue (PB27) modified with polyorganosiloxane (POS) grafted with (**a**) poly(acrylic acid) (PAA) (PB27@POS@PAA) or (**b**) poly(N-(2-hydroxyethyl) acrylamide) (PHEAA) (PB27@POS@PHEAA) at 90 °C and 18 °C.

TGA was then used to study the thermal stability in a wide temperature range of the functional composite pigment particles, as shown in Figure 8. PB27 was partly decomposed at a low temperature near 150 °C, which is ascribed to the bound water. There were another two decomposition stages at temperatures 350 °C and 650 °C, leading to a total weight loss of 58%. Comparably, there was a gradual weight loss for PB27@POS and a total weight loss of 36.8%, mainly due to the decomposition of organic components of POS, without low-temperature degradation below 200 °C and high-temperature degradation near 650 °C, indicating that the thermal stability was greatly enhanced after

encapsulating PB27 with POS. For PB27@POS@PAA-400, two weight loss peaks appeared with a total weight loss of 76.8%. The first stage of mass loss was mainly due to the decomposition of PAA. The second stage of mass loss was probably attributed to the decomposition of POS, indicating that the polymer grafting may reduce the thermostability of POS but have no effect on PB27. Similarly, for PB27@POS@PHEAA-400, there was a 74.8% mass loss from 50 °C to 480 °C, which was mainly due to the decomposition of PHEAA. And the 14.4% mass loss between 480 °C and 800 °C was due to the decomposition of POS.

As shown in Figure 8, the residual mass of PB27 is 42% after heating to 800 °C. After encapsulation, the residual masses are 23.2% for PB27@POS@PAA-400 and 10.8% for PB27@POS@PHEAA-400. As calculated, 98% HEAA was grafted on the surface of PB27@POS and 87% AA was grafted on the surface of PB27@POS, demonstrating a high conversion by this simple preparation strategy.

Figure 8. (**a**) TGA and (**b**) DTG of Prussian blue (PB27), PB27 modified with polyorganosiloxane (POS) (PB27@POS), and grafted with poly(acrylic acid) (PAA) (PB27@POS@PAA) or poly(N-(2-hydroxyethyl) acrylamide) (PHEAA) (PB27@POS@PHEAA).

3.4.2. Mechanical Stability

To explore the centrifugation effect on the mechanical stability of the functional composite pigment particles with different brush thicknesses, the optical photos and the particle size of the samples involved were recorded and measured, as shown in Figures 9 and 10. In Figure 9, the color turned dark with increased brush thickness. The color fading for samples with thin brush thickness is ascribed to the sediment of unstable particles. The thicker the polymer brushes (PAA or PHEAA), the better the mechanical stability of the particles. The thicker the polymer brushes, the more hydrophilic hydroxyl groups or carboxyl groups, and the better the affinity with the water phase, the lighter the settlement.
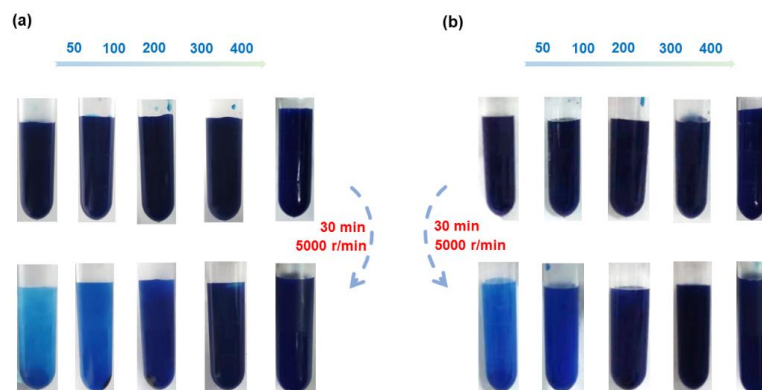
Figure 9. Optical photos of the functional composite pigment particles composed of Prussian blue (PB27) modified with polyorganosiloxane (POS) grafted with (**a**) poly(acrylic acid) (PAA) (PB27@POS@PAA) or (**b**) poly(N-(2-hydroxyethyl) acrylamide) (PHEAA) (PB27@POS@PHEAA) with different brush thicknesses before and after centrifugation.
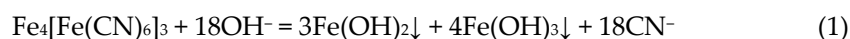
As shown in Figure 10, the particle size of PB27@POS@PAA-200, PB27@POS@PAA-300, PB27@POS@PAA-400, PB27@POS@PHEAA-200, PB27@POS@PHEAA-300, or PB27@POS@PHEAA-400 with thicker polymer brushes showed less size variation. That of PB27@POS@PAA with thicker polymer brushes is less than that of PB27@POS@PHEAA, which benefits from the electrostatic repulsion between PAA chains. The particle size of PB27@POS@PAA-50, PB27@POS@PAA-100, PB27@POS@PHEAA-50, or PB27@POS@PHEAA-100 with thinner polymer brushes decreased significantly, which may be attributed to the visible sedimentation in these samples at the same centrifugal speed.
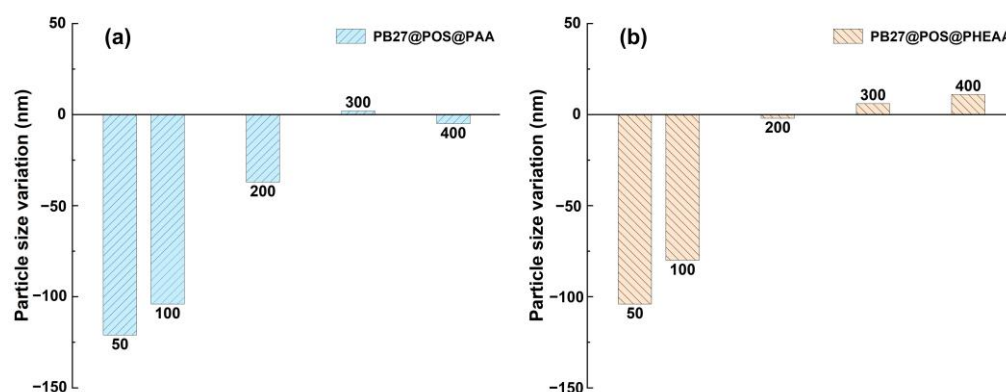
Figure 10. The particle size variation in Prussian blue (PB27) modified with polyorganosiloxane (POS) grafted with (**a**) poly(acrylic acid) (PAA) (PB27@POS@PAA) or (**b**) poly(N-(2-hydroxyethyl) acrylamide) (PHEAA) (PB27@POS@PHEAA) after centrifugation (5000 rpm, 30 min).

3.4.3. Alkali Resistance

The color of PB27 varies when it is decomposed by alkali. The changes in the color of the sample solutions with time were recorded to analyze the effect of polymer brushes on the alkali resistance of PB27. It can be observed in Figure 11a, that PB27 in an alkaline environment changed its color over time from blue to green to orange and the color of PB27@POS@PAA-50 and PB27@POS@PAA-100 gradually went from blue to dark green to orange over time. The color change may be closely related to $Fe(OH)_2$ and $Fe(OH)_3$, which originates from the following equation. The $Fe(OH)_2$ produced by the decomposition of PB27 by alkali was adsorbed on the surface of the composite pigment particles, showing a green color. The oxidation of $Fe(OH)_2$ and the further decomposition of PB27 generated more and more $Fe(OH)_3$, giving the sample solution an orange–yellow color. PB27@POS@PAA-200 maintained a good blue hue for 8 h. This could be ascribed to the fact that thicker polymer brushes digested more OH^- and thicker polymer brushes equipped the composite pigment particles with stronger steric hindrance. However, with AA dosage further increased, the color of PB27@POS@PAA-300 and PB27@POS@PAA-400 also changed dramatically. This may be brought by the enhanced ion osmotic effect dominated. Driven by osmotic pressure, OH^- entered the inner layer of the polymer brushes, thus decomposing PB27 quickly.

$$Fe_4[Fe(CN)_6]_3 + 18OH^- = 3Fe(OH)_2\downarrow + 4Fe(OH)_3\downarrow + 18CN^- \tag{1}$$

$$4Fe(OH)_2 + O_2 + 2H_2O = 4Fe(OH)_3\downarrow \tag{2}$$

The color changes in PB27@POS@PHEAA mixed with NaOH solution (0.25 M) are shown in Figure 11b. In contrast with PB27@POS@PAA, its color changed more regularly.

The color of PB27@POS@PHEAA-50, PB27@POS@PHEAA-100, and PB27@POS@PHEAA-200 all transferred from blue to dark green to light green to orange in a period (0, 1, 2, 3 h). The color of PB27@POS@PHEAA-300 solution changed from dark blue to light blue to light green, and that of PB27@POS@PHEAA-400 changed from dark blue to light blue to lime green. Comparably, PB27@MPPOS@PHEAA-300 and PB27@MPPOS@PHEAA-400 have better alkaline resistance. The brushes thicknesses of PB27@POS@PHEAA-300 and PB27@POS@PHEAA-400 are thicker, making it harder for OH⁻ to contact and decompose PB27 [43].
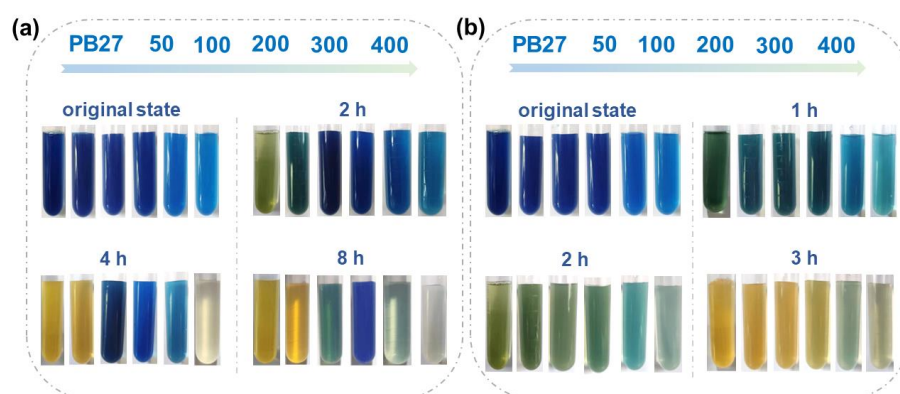
Figure 11. Pictures of (**a**) Prussian blue (PB27) modified with polyorganosiloxane (POS) grafted with poly(acrylic acid) (PAA) (PB27@POS@PAA) solutions mixed with NaOH solution in a period of time (0, 2, 4, and 8 h) and those of (**b**) Prussian blue (PB27) modified with polyorganosiloxane (POS) grafted with poly(N-(2-hydroxyethyl) acrylamide) (PHEAA) (PB27@POS@PHEAA) solutions mixed with NaOH solution in a period of time (0, 1, 2, and 3 h).

The particle size data along with the alkali resistance test measured by DLS are shown in Figure 12. The particle size of PB27 gradually decreased due to its decomposition by OH⁻. For brush-like composite pigment particles with different PAA thicknesses, the particle size variation decreased gradually as the amount of AA increased from 50 wt% to 200 wt%. As the amount of AA increased from 200 wt% to 400 wt%, the particle size changed more fiercely. PB27@POS@PAA-200 showed better alkaline resistance. In terms of brush-like composite pigment particles with different PHEAA thicknesses, as the amount of HEAA increased from 50 wt% to 400 wt%, the thicker the PHEAA thickness, the weaker the particle variation. The particle size of PB27@POS@PHEAA-400, which showed the best alkaline resistance, decreased from the initial 415 nm to 220 nm after 3 h. In contrast, the particle size of PB27@POS@PAA-200 could be reduced by only 31 nm in 8 h, which had better alkaline resistance.
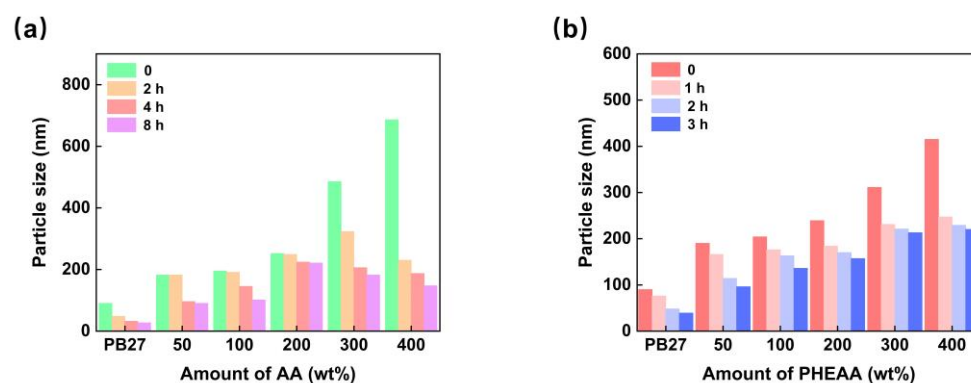
Figure 12. Particle size of (**a**) Prussian blue (PB27) modified with polyorganosiloxane (POS) grafted with poly(acrylic acid) (PAA) (PB27@POS@PAA) solutions mixed with NaOH solution in a period of time (0, 2, 4, and 8 h) and those of (**b**) Prussian blue (PB27) modified with polyorganosiloxane

(POS) grafted with poly(N-(2-hydroxyethyl) acrylamide) (PHEAA) (PB27@POS@PHEAA) solutions mixed with NaOH solution in a period of time (0, 1, 2, and 3 h).

PHEAA is a nonionic polymer and it is not able to consume part of the OH⁻ or respond to pH as PAA chains do in an alkaline environment. Therefore, in terms of improving the alkali resistance of PB27, PB27@POS@PHEAA behaved worse than PB27@POS@PAA. The alkaline resistance of PB27@POS@PHEAA is mainly dependent on the thickness of the polymer brushes. In a word, the type of polymer brush and the brush thickness are closely related to the alkali resistance of PB27.

3.5. Functionality

3.5.1. pH Response of PB27@POS@PAA

DLS information of PB27@POS@PAA at different pH values indicates that they all have a good pH-stimuli response. As shown in Figure 13, the sizes increased with pH due to the deprotonation of PAA chains. The difference is the particle size variation range of PB27@POS@PAA with pH. The thicker the brush thickness, the bigger the particle size variation and the more obvious the pH response. At pH < 4, the PAA chains collapsed completely on the surface of PB27@POS because the electrostatic repulsion between the PAA chains was greatly reduced. Especially for PB27@POS@PAA-50, its particle size was nearly the same as that of PB27@POS. At pH > 8, there was a larger electrostatic repulsion between the negatively charged chains as the PAA chains ionized more H⁺, contributing to the constant stretching of PAA chains in space. It can also be seen from Figure 12 that there was no specific relationship between PDI and pH, indicating that PDI had no pH response.

For most applications involving coatings, the pH is maintained around pH 9.5, in which better stability would be obtained for PB27@POS@PAA due to enhanced electrostatic repulsion. Moreover, the abundant carboxyl groups in the PAA chain could provide active sites for further functionality like luminescence by fluorescent molecules.
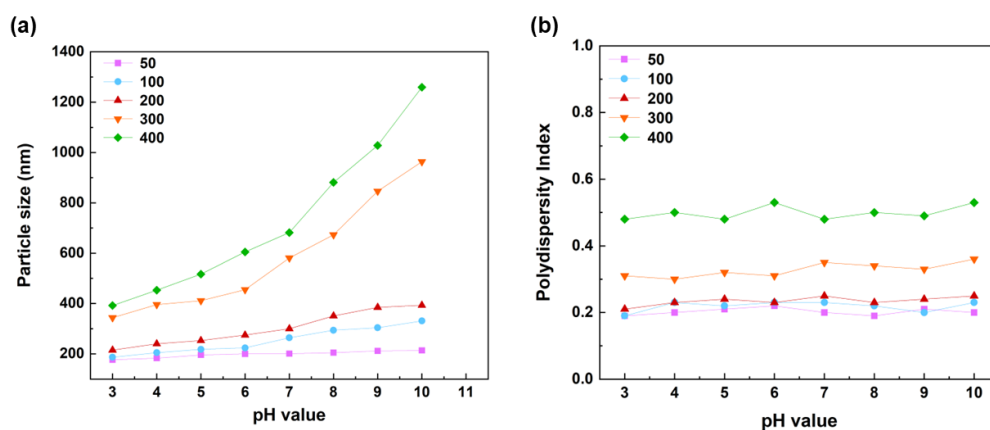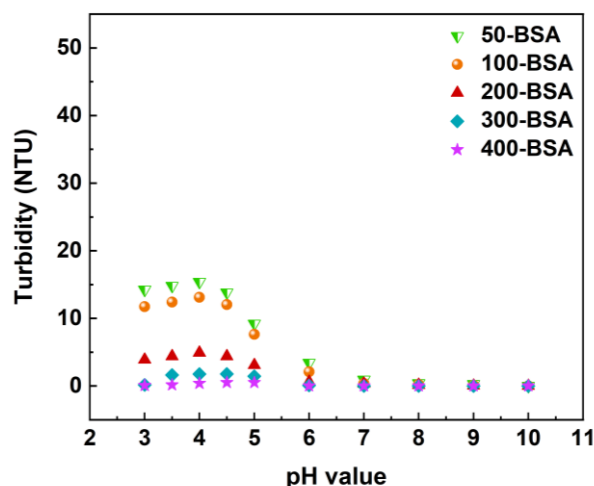

Figure 13. (**a**) Particle size and (**b**) size distribution of Prussian blue (PB27) modified with polyorganosiloxane (POS) grafted with poly(acrylic acid) (PAA) (PB27@POS@PAA) with pH.

#### 3.5.2. Antifouling Property of PB27@POS@PHEAA

For biological fouling, protein adsorption is crucial to the adhesion of microorganisms on the surfaces. In this work, bovine serum albumin protein (BSA, p*I* 4.9) was chosen as the model protein to study the antifouling property of PB27@POS@PHEAA. Both turbidimeter and DLS were applied. The interaction between BSA and PB27@POS without HEAA feeding was too fierce to characterize so it was not involved. As shown in Figure 14, the turbidity of the mixture of PB27@POS@PHEAA-50 and BSA rose dramatically. Similarly, the turbidity of the mixture of PB27@POS@PHEAA-100 and BSA also increased

significantly, suggesting obvious adsorption of BSA. Comparably, PB27@POS with 200 wt%, 300 wt%, and 400 wt% HEAA dosage showed slighter growth in turbidity corresponding to a good antifouling property, which could be ascribed to the hydrated layer in PHEAA structure with high resistance to nonspecific protein adsorption, indicating that high grafting of PHEAA was effective for antifouling. This could be ascribed to thicker polymer brushes with stronger steric hindrance, making nonspecific protein adsorption to PB27@POS@HEAA more difficult. The turbidity of PB27@POS@PHEAA and that of blank BSA were shown in the supporting information (Figure S2).

Figure 14. The turbidity of Prussian blue (PB27) modified with polyorganosiloxane (POS) grafted with poly(N-(2-hydroxyethyl) acrylamide) (PHEAA)-bovine serum albumin protein (PB27@POS@PHEAA-BSA) with pH.

The particle size was also measured by DLS along with the turbidity titration test and the result is shown in Figure 15. In contrast with PB27@POS@PAA, whose particle size varied regularly through the pH, the particle size of PB27@POS@PHEAA varied less with pH, indicating that PB27@POS@PHEAA was stable to pH. In Figure 15, the size of the mixture of BSA and PB27@POS@PHEAA-200, PB27@POS@PHEAA-300, or PB27@POS@PHEAA-400 maintained a constant pH. However, the size variation is bigger for that of PB27@POS@PHEAA-50 and PB27@POS@PHEAA-100, which is consistent with the turbidity result.
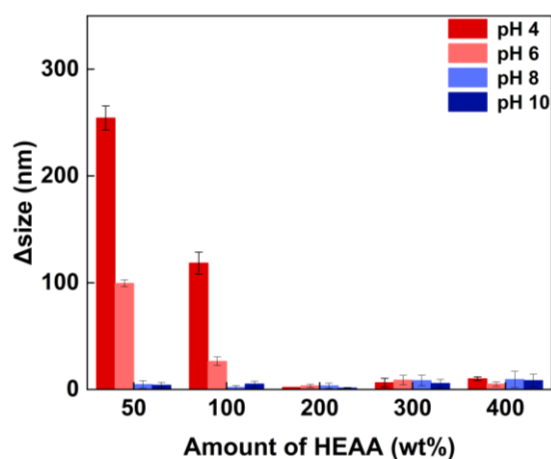
Figure 15. The particle size variation in Prussian blue (PB27) modified with polyorganosiloxane (POS) grafted with poly(N-(2-hydroxyethyl) acrylamide) (PHEAA)-bovine serum albumin protein (PB27@POS@PHEAA-BSA) at a certain pH.

Hydrophilicity is one of the important factors in the adsorption resistance of polymers. PHEAA is a kind of hydrophilic polymer rich in hydroxyl groups. In this work, the hydrophilic PHEAA polymer was successfully grafted onto the PB27@POS surface by a simple grafting method. The antifouling analyses of PB27@POS@PHEAA at different pH values implied that PB27@POS@PHEAA-200, PB27@POS@PHEAA-300, and PB27@POS@PHEAA-400 had better resistance to nonspecific protein adsorption and that these functional composite pigment particles have bright prospects in applications with antibacterial and antifouling properties.

Two different functional polymers, i.e., PAA and PHEAA, were introduced to the PB27@POS surface, endowing different functions including enhanced stability. The proposed strategy herein provides a versatile way to modify pigments and further bring possible functionalization according to requirements.

4. Conclusions

In this work, it was found that the grafting polymerization of functional polymer on the surface of Prussian blue (PB27) modified with polyorganosiloxane (POS) (PB27@POS) can be controlled by changing the dosage of the grafted monomers or the initiator potassium persulfate (KPS). Optimal mechanical stability could be obtained for brush-like composite pigment particles after centrifuging under 5000 rpm in 30 min and good thermostability treated under 90 °C appeared when the dosage of grafting monomer AA or HEAA reached 400 wt%. In terms of alkali resistance, Prussian blue (PB27) modified with polyorganosiloxane (POS) grafted with poly(acrylic acid) (PAA) (PB27@POS@PAA) (AA, 200 wt%) could maintain a good blue hue for 8 h and its particle size variation was only 31 nm after 8 h. Comparably, Prussian blue (PB27) modified with polyorganosiloxane (POS) grafted with poly(N-(2-hydroxyethyl) acrylamide) (PHEAA) (PB27@POS@PHEAA) behaved worse than PB27@POS@PAA. Not only the hue of PB27@POS@PHEAA turned a lot but also its particle size decreased by 195 nm after 3 h with similar conditions. PB27@POS@PAA exhibited an obvious pH response and good antifouling property was obtained for PB27@POS@PHEAA with higher HEAA dosage. This work provides a novel strategy to fabricate functional and well-dispersed composite PB27 particles based on polyorganosiloxane, which can be extended to other polymers like modified POS, polyacrylics, etc., which has potential applications in coatings and inks fields with extreme application conditions.

References

1. Mahltig, B.; Zhang, J.; Wu, L.; Darko, D.; Wendt, M.; Lempa, E.; Rabe, M.; Haase, H. Effect pigments for textile coating: A review of the broad range of advantageous functionalization. *J. Coat. Technol. Res.* **2017**, *14*, 35–55.
2. Ali, M.; Lin, L.; Cartridge, D. High electrical conductivity waterborne inks for textile printing. *J. Coat. Technol. Res.* **2019**, *16*, 1337–1349.
3. Varney, D.; Toivakka, M.; Bousfield, D. Discrete element method to predict the mechanical properties of pigmented coatings. *J. Coat. Technol. Res.* **2019**, *16*, 1683–1689.
4. Nie, L.; Chang, G.; Li, R. Preparation and Characterization of Self-Dispersing Phthalocyanine Blue 15:4 Pigment for Dyeing of Wool Textiles. *Coatings* **2020**, *10*, 741.
5. Nie, L.; Dong, Y.; Chen, Y.; Chang, G.; Li, R. A study for self-dispersing pigment-based inks printing on various fabrics. *Colloids Surf. A* **2023**, *658*, 130689.
6. Gong, L.; Hua, X.; Yao, B.; Liang, J.; Tian, G. Novel red composite pigment with high thermostability from iron ore tailings: Synthesis and coloring mechanism. *Ceram. Int.* **2023**, *49*, 5066–5076.
7. Men, P.; Liang, J.; He, J.; Chen, J.; Geng, B.; Li, W. Preparation of alkali-resistant aluminum pigment encapsulated with fluoro-polymer by in situ polymerization. *J. Coat. Technol. Res.* **2021**, *18*, 1227–1235.
8. Marzec, A.; Szadkowski, B. Improved Aging Stability of Ethylene-Norbornene Composites Filled with Lawsone-Based Hybrid Pigment. *Polymers* **2019**, *11*, 723.
9. Karangutkar, A.V.; Ananthanarayan, L. Evaluating the effect of additives on stability of betacyanin pigments from Basella rubra in a model beverage system during storage. *J. Food Sci. Technol. Mysore* **2021**, *58*, 1262–1273.
10. Lv, D.; Sung, H.-S.; Li, X.; Zhang, X.; Li, Z.; Chen, D. Effects of single layer graphene and graphene oxide modification on the properties of phthalocyanine blue pigments. *Dye. Pigm.* **2020**, *180*, 108449.
11. Hakeim, O.A.; Arafa, A.A.; Zahran, M.K.; Dou, L.A.W. UV-curable encapsulation of surface Modified organic pigments for inkjet printing of textiles. *Colloids Surf. A* **2014**, *447*, 172-182.
12. Kozlowska, M.; Lipinska, M.; Okraska, M.; Pietrasik, J. Polypropylene Color Masterbatches Containing Layered Double Hydroxide Modified with Quinacridone and Phthalocyanine Pigments-Rheological, Thermal and Application Properties. *Materials* **2023**, *116*, 6243.
13. Ren, F.; Fei, X.; Cui, L.; Cao, L.; Lv, D.; Zhu, S.; Han, X.; Liu, L. Preparation and properties of hydrophilic PR 57:1 with inorganic core/solid solution shell. *Dye. Pigm.* **2020**, *183*, 108699.
14. Chen, X.-H.; Tang, C.-H. Highly transparent antioxidant high internal phase emulsion gels stabilized solely by C-phycocyanin: Facilitated formation through subunit dissociation and refractive index matching. *Colloids Surf. A* **2021**, *625*, 126866.
15. Win, K.Y.; Teng, C.P.; Tee, S.Y.; Guan, G.; Loh, X.J.; Han, M.-Y. Natural polymer towards lustrous multicolored silk: Hermetical encapsulation and understanding of colorants via controlled de/recrystallization process. *Polymer* **2021**, *233*, 124163.
16. Chen, Y.; Li, X.; Luan, Z.; Zhu, L.; Hu, J.; Xia, X.; Ma, K.; Geng, B.; Yan, M. Fabrication of intelligent anticorrosion waterborne aluminum pigments based on encapsulation of composited zeolitic imidazole framework layers. *J. Mater. Sci.* **2023**, *58*, 8143–8156.
17. Nguyen, D.; Huynh, V.; Lam, M.; Serelis, A.; Davey, T.; Paravagna, O.; Such, C.; Hawkett, B. Encapsulation by Directed PISA: RAFT-Based Polymer-Vesiculated Pigment for Opacity Enhancement in Paint Films. *Macromol. Rapid Commun.* **2024**, *42*, 2100008.
18. Liu, L.; Zhou, Y.; Chen, K.; Gan, W.; Wen, S.; Wang, B. Structural design and preparation of pigment/resin integrated ultra-stable antibacterial composite particles. *Dye. Pigm.* **2022**, *201*, 110242.
19. Zhou, Y.; Chen, K.; Liu, L.; Wen, S.; Gui, T. The Design and Preparation of Antibacterial Polymer Brushes with Phthalocyanine Pigments. *Coatings* **2023**, *13*, 1114.
20. Zhang, L.; Shao, G.; Xu, R.; Ding, C.; Hu, D.; Zhao, H.; Huang, X. Multicovalent crosslinked double-network graphene-polyorganosiloxane hybrid aerogels toward efficient thermal insulation and water purification. *Colloids Surf. A.* **2022**, *647*, 129129.
21. Liu, H.; Zhang, Y.; Ma, Z.; Zhang, H. Robust surface with thermally stable hydrophobicity enabled by electrosprayed fluorinated SiO2 particles. *J. Coat. Technol. Res.* **2022**, *19*, 347-353.
22. Yang, F.; Zhu, L.; Han, D.; Li, W.; Chen, Y.; Wang, X.; Ning, L. Effects of fluorine and silicon components on the hydrophobicity failure behavior of acrylic polyurethane coatings. *J. Coat. Technol. Res.* **2017**, *14*, 691–699.
23. Qian, H.; Jiang, B. Silicone Resin Applications for Heat-Resistant Coatings: A Review. *Polym. Sci. Ser. C Sel. Top.* **2023**, *65*, 143–145.
24. Mathew, A.; Kurmvanshi, S.; Mohanty, S.; Nayak, S.K. Sustainable production of polyurethane from castor oil, functionalized with epoxy- and hydroxyl-terminated poly(dimethyl siloxane) for biomedical applications. *J. Mater. Sci.* **2018**, *53*, 3119–3130.
25. Smith, G.N.; Brok, E.; Schmiele, M.; Mortensen, K.; Bouwman, W.G.; Duif, C.P.; Hassenkam, T.; Alm, M.; Thomsen, P.; Arleth, L. The microscopic distribution of hydrophilic polymers in interpenetrating polymer networks (IPNs) of medical grade silicone. *Polymer* **2021**, *224*, 123671.
26. Lv, S.; Zhang, X.; Yang, X.; Xu, Q.; Chen, G.; Liu, X.; Yang, Z.; Zhai, Y. Slippery surface for enhancing surface robustness and chemical stability. *J. Mater. Sci.* **2023**, *58*, 5837–5847.
27. Jadhav, S.A.; Bongiovanni, R.; Marchisio, D.L.; Fontana, D.; Egger, C. Surface modification of iron oxide (Fe2O3) pigment particles with amino-functional polysiloxane for improved dispersion stability and hydrophobicity. *Pigment Resin Technol.* **2014**, *43*, 219–227.

28. Xie, Z.; Yan, X.; Li, J.; Zhu, C.; Qi, D. Pigment printing of polyester fabric using a single step synthesized PDMS-modified poly-urethane-acrylic/pigment hybrid emulsion. *Text. Res. J.* **2022**, *92*, 2818–2829.
29. Wang, F.; Li, J.; Lu, L.; Yan, X.; Qi, D.; Chen, Z. One-step mini-emulsion copolymerisation of waterborne polysiloxane-modified polyacrylate/pigment hybrid latex and its application in textile pigment printing. *Color. Technol.* **2022**, *138*, 291–303.
30. Zhang, Q.; Wu, M. Structure of vinyl polysiloxane on properties of polyacrylates film and its pigment printing application. *J. Coat. Technol. Res.* **2020**, *17*, 937-948.
31. Meng, C.; Cao, Y.; Sun, L.; Liu, Y.; Kang, G.; Ma, W.; Peng, J.; Deng, K.; Ma, L.; Wei, H. Synthesis of cyclic graft polymeric prodrugs with heterogeneous grafts of hydrophilic OEG and reducibly conjugated CPT for controlled release. *Biomater. Sci.* **2020**, *8*, 4206–4215.
32. Duan, M.; Chen, G. Swelling and shrinking of two opposing polyelectrolyte brushes. *Phys. Rev. E* **2023**, *107*, 024502.
33. Bauman, L.; Wen, Q.; Sameoto, D.; Yap, C.H.; Zhao, B. Durable poly(N-isopropylacrylamide) grafted PDMS micropillared sur-faces for temperature-modulated wetting. *Colloids Surf. A* **2021**, *610*, 125901.
34. Jana, S.; Ray, J.; Mondal, B.; Pradhan, S.S.; Tripathy, T. pH responsive adsorption/desorption studies of organic dyes from their aqueous solutions by katira gum-cl-poly(acrylic acid-co-N-vinyl imidazole) hydrogel. *Colloids Surf. A* **2018**, *553*, 472-486.
35. Dai, X.; Xu, X.; Yu, X.; Sun, X.; Pan, J.; Zhang, X.; Min, J. Cationic core/shell polysiloxane acrylate emulsion: Synthesis, film morphology, and performance on cotton pigment coloration. *Cellulose* **2022**, *29*, 2093–2106.
36. Shen, J.; Hu, Y.; Li, L.-X.; Sun J-w Kan, C.-Y. Fabrication and characterization of polysiloxane/polyacrylate composite latexes with balanced water vapor permeability and mechanical properties: Effect of silane coupling agent. *J. Coat. Technol. Res.* **2018**, *15*, 165–173.
37. Zhou, X.; Zhang, C.; Zhou, Q.; Liang, J.; Zhang, X.; Shi, Y.; Zhu, J.; Zhong, L. Imaging application of an MMP2-sensitive tumor-targeted prussian blue fluorescent nanoprobe. *J. Biomater. Appl.***2023**, *38*, 372-380.
38. Zhou, M.; Tian, X.; Sun, Y.; He, X.; Li, H.; Ma, T.; Zhao, Q.; Qiu, J. Pillar effect boosting the electrochemical stability of Prussian blue-polypyrrole for potassium ion batteries. *Nano Res.* **2023**, *16*, 6326–6333.
39. Dwivedi, C.; Kumar, A.; Singh, K.K.; Juby, A.K.; Kumar, M.; Wattal, P.W.; Bajaj, P.N. Copper hexacyanoferrate–polymer com-posite beads for cesium ion removal: Synthesis, characterization, sorption, and kinetic studies. *J. App. Polym. Sci.* **2013**, *129*, 152–160.
40. Parajuli, D.; Tanaka, H.; Sakurai, K.; Hakuta, Y.; Kawamoto, T. Thermal Decomposition Behavior of Prussian Blue in Various Conditions. *Materials* **2021**, *14*, 1151.
41. Salatiello, S.; Spinelli, M.; Cassiano, C.; Amoresano, A.; Marini, F.; Cinti, S. Sweat urea bioassay based on degradation of Prus-sian Blue as the sensing architecture. *Anal. Chim. Acta* **2022**, *1210*, 339882.
42. Wang, Z.; Chen, K.; Hua, C.; Guo, X. Conformation variation and tunable protein adsorption through combination of poly(acrylic acid) and antifouling poly(N-(2-hydroxyethyl) acrylamide) diblock on a particle surface. *Polymers* **2020**, *12*, 566.
43. Hua, C.; Chen, K.; Wang, Z.; Guo, X. Preparation, stability and film properties of cationic polyacrylate latex particles with vari-ous substituents on the nitrogen atom. *Prog. Org. Coat.* **2020**, *143*, 105628.